ADVANCED OXIDATION TECHNOLOGIES: STATE-OF-THE-ART IN IBERO-AMERICAN COUNTRIES

CrossMark

Degradation of ampicillin antibiotic by electrochemical processes: evaluation of antimicrobial activity of treated water

Jorge Vidal[1] · Cesar Huiliñir[2] · Rocío Santander[1] · Javier Silva-Agredo[3] · Ricardo A. Torres-Palma[3] · Ricardo Salazar[1]

Abstract

Ampicillin (AMP) is an antibiotic widely used in hospitals and veterinary clinics around the world for treating infections caused by bacteria. Therefore, it is common to find traces of this antibiotic in wastewater from these entities. In this work, we studied the mineralization of this antibiotic in solution as well as the elimination of its antimicrobial activity by comparing different electrochemical advanced oxidation processes (EAOPs), namely electro-oxidation with hydrogen peroxide (EO-H_2O_2), electro-Fenton (EF), and photo electro-Fenton (PEF). With PEF process, a high degradation, mineralization, and complete elimination of antimicrobial activity were achieved in 120-min electrolysis with high efficiency. In the PEF process, fast mineralization rate is caused by hydroxyl radicals ($\cdot$OH) that are generated in the bulk, on the anode surface, by UV radiation, and most importantly, by the direct photolysis of complexes formed between Fe^{3+} and some organic intermediates. Moreover, some products and intermediates formed during the degradation of the antibiotic Ampicillin, such as inorganic ions, carboxylic acids, and aromatic compounds, were determined by photometric and chromatographic methods. An oxidation pathway is proposed for the complete conversion to CO_2.

Keywords Degradation of ampicillin, antimicrobial activity decay · Photoelectro-Fenton process, hydroxyl radical · Mineralization

✉ Ricardo Salazar
ricardo.salazar@usach.cl

[1] Laboratorio de Electroquímica del Medio Ambiente (LEQMA), Departamento de Química de los Materiales, Facultad de Química y Biología, Universidad de Santiago de Chile (USACH), Casilla 40, Correo, 33 Santiago, Chile

[2] Departamento de Ingeniería Química. Laboratorio de Biotecnología Ambiental, Facultad de Ingeniería, Universidad de Santiago de Chile (USACH), Santiago, Chile

[3] Grupo de Investigación en Remediación Ambiental y Biocatálisis (GIRAB), Instituto de Química, Facultad de Ciencias Exactas y Naturales, Universidad de Antioquia (UdeA), Calle 70 No 52-21, Medellín, Colombia

Introduction

Ampicillin is a β-lactam antibiotic that belongs to the penicillin family. This drug is used to treat some infections caused by bacteria, such as meningitis, infections in the lungs, blood, heart, urinary tract, and gastrointestinal tract (Katzung et al. 2013; Serna-Galvis et al. 2016a, b). Due to its broad spectrum of application, this antibiotic can be found in different sources such as hospitals, veterinary, and domestic wastewater (Kemper 2008; Kummerer 2009).

Antibiotics, in general, are very difficult to remove by conventional biological and chemical treatments. Their photoresistance and low biodegradability have made them attract the attention of the scientific community (Feng et al. 2013; Serna-Galvis et al. 2015; Sirés and Brillas 2016), which has made considerable efforts to find the right treatment to remove these emergent pollutants from wastewater. During the last 20 years, different researchers have proved that an

excellent alternative to eliminate emergent and/or persistent organic pollutants is electrochemical advanced oxidation processes (EAOPs) (Masomboon et al. 2010; Salazar et al. 2011; García-Segura et al. 2017).

EAOPs are processes that use electricity to electroproduce in situ strong oxidizing agents like hydroxyl radical (·OH) (Moreira et al. 2014). ·OH has a high standard potential (E° = 2.80 V vs SHE) that makes it capable of non-selectively reacting with organics to produce hydroxylated or dehydrogenated derivatives, until their complete mineralization to CO_2, water, and inorganic ions (Sales Solano et al. 2015).

Among EAOPs is electrochemical oxidation, in which pollutants are oxidized by heterogeneous M(·OH) formed from water discharge at the anode surface and at high current, as shown by Eq. (1) (García-Segura et al. 2016a, b; Pérez et al. 2017a, b).

$$M + H_2O \rightarrow M(\bullet OH) + e^- + H^+ \qquad (1)$$

$$O_2 + 2H^+ + 2e^- \rightarrow H_2O_2 \qquad (2)$$
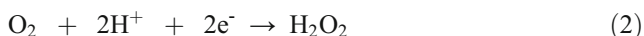
Other EAOP, which is based on Fenton reaction chemistry used for the decontamination of water, is EF. In this treatment, H_2O_2 is continuously electrogenerated (Eq. (2)) at a carbonaceous cathode and reacts with a small concentration of Fe^{2+} that is added to the solution to yield Fe^{3+} ion and homogeneous ·OH in the bulk ((Eq. (3)), with optimum pH 2.8 (Abdessalem et al. 2010; Annabi et al. 2016). The advantages of EF over the classical Fenton reagent treatment are the in situ generation of H_2O_2 and the cathodic generation of Fe^{2+} ion from the reduction of Fe^{3+} generated in the Fenton's Eq. (4), thereby accelerating Fenton Eq. (3) and enhancing the mineralization process (de Luna et al. 2012; Olvera-Vargas et al. 2015; Pereira et al. 2016).

$$Fe^{2+} + H_2O_2 \rightarrow \bullet OH + Fe^{3+} + {}^-OH \qquad (3)$$

$$Fe^{3+} + e^- \rightarrow Fe^{2+} \qquad (4)$$
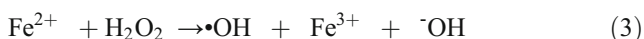
On the other hand, to increase the rate of degradation and mineralization of the organic compounds in solution in the EF process, it is possible to irradiate the system with a UV light (García-Segura et al. 2012; Liu et al. 2013; Bedolla-Guzmán et al. 2016). This process is known as PEF. With direct irradiation, the efficiency of the method is higher than that of EF because of (i) further regeneration of Fe^{2+} and production of homogeneous ·OH radicals from the photoreduction of $Fe(OH)^{2+}$ (Eq. (5)) (Babuponnusami and Muthukumar 2012; García-Rodríguez et al. 2016):

$$Fe(OH)^{2+} + hv \rightarrow Fe^{2+} + \bullet OH \qquad (5)$$

(ii) photo decarboxylation of iron(III) complexes with intermediates carboxylic acids generated by the action of the hydroxyl radical on the organic pollutant, according to Eq. (6) (Anotai et al. 2011; Díez et al. 2016):

$$Fe(OOCR)^{2+} + hv \rightarrow Fe^{2+} + CO_2 + R\bullet \qquad (6)$$
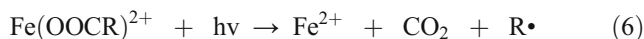
This last process may be complemented with a method that has been studied by our research group, which consists in EO-H_2O_2 using an anode, specifically, a boron-doped diamond (BDD) (Espinoza et al. 2016; Vidal et al. 2016). This anode interacts very weakly with physisorbed BDD(·OH) produced from Eq. (7) and promotes a much greater O_2-overpotential than other conventional anodes like Pt to achieve the removal of organics (El-Ghenymy et al. 2015; Zazou et al. 2016). In this process, the organic contaminant may undergo two simultaneous oxidations: (i) oxidation from the ·OH formed in the solution according to the Fenton reaction (Eq. (3)) and (ii) oxidation by the action of ·OH surface (M) through the discharge of water according to Eq. (7) (García-Segura et al. 2013; Benito et al. 2017; Cruz-Rizo et al. 2017):

$$BDD + H_2O \rightarrow BDD(\bullet OH) + e^- + H^+ \qquad (7)$$

In the present study, the main objective was to compare different electrochemical advanced oxidation for the degradation, mineralization, and evaluation of the removal of the antimicrobial activity of the antibiotic ampicillin in water.

Experimental methods

Reagents

Sodium ampicillin (CAS number: 69-52-3, $C_{16}H_{18}N_3NaO_4S$, 99.9% of purity) was supplied by Sigma-Aldrich® and was used as received. The chemical structure and some characteristics of the antibiotic are shown in SM1. Analytical grade oxamic and malic acids were from Sigma-Aldrich®, while oxalic, maleic, formic, and acetic were from Merck®. Solutions of anhydrous sodium sulfate (used as supporting electrolyte) and iron sulfate II heptahydrate (analytical grade from Merck) were prepared with distilled water and had their pH adjusted with analytical grade sulfuric acid or sodium hydroxide (both from Merck). Hydrogen peroxide was provided by Sigma-Aldrich®. Milli-Q water, acetonitrile (Merck, HPLC grade) and methanol (J.T.BAKER, HPLC grade) were used for the preparation of the HPLC mobile phase.

Electrochemical system

Electrochemical experiments for ampicillin (AMP) degradation were carried out in a 250-mL, one-compartment electrolytic cell. Galvanostatic electrolyses were performed with an MCP model M10-QD305 power supply, which displayed the current and voltage. A carbon-PTFE air diffusion electrode

was used as cathode. The preparation of the air diffusion electrode has been reported in other studies (Chávez et al. 2010). A boron-doped diamond electrode (BDD) was used as anode with a 2.75-mm thick p-doped diamond layer with a concentration of 500 ppm of boron supplied by Adamant®. Both electrodes with a geometric area of 5 cm^2 and separated from each other by 1 cm. All experiments contained 0.05 M Na$_2$SO$_4$ as supporting electrolyte with a concentration of 1 mg L^{-1} of Fe^{2+} at pH 2.8 under constant stirring conditions. The effect of the applied current density (j) was tested at 2, 5, 20, and 50 mA cm^{-2} and the effect of the initial concentration of AMP in solution was studied at 10, 50, 75, and 100 mg L^{-1} in addition to an experiment in micromolar concentration (10 and 50 μg L^{-1}). In PEF assays, the solution was irradiated with a fluorescent black light blue tube (λ_{max} = 360 nm, 5.0 W m^{-2}) placed in the center of electrochemical cell were is added the solution.

The removal of AMP was performed in a real industrial wastewater from a Slaughterhouse company located in the town of Puente Alto, Santiago of Chile. The company provides a full service to slaughterhouse and roughing of pork and beef, and treats its effluents generated from the production in accordance with Chilean standards. For these experiments, wastewater samples where collected after primary and secondary treatment of the plant (decantation, coagulation, and aerobic biological treatment), in March 20th, 2018. Two hundred fifty milliliters of industrial wastewater was spike with 50 mg L^{-1} of AMP and treated by PEF applying a current density of 5 mA cm^{-2}, in the presence of 1 mg L^{-1} of Fe^{2+} and 0.05 M Na$_2$SO$_4$ at pH 2.8 and 30 °C.
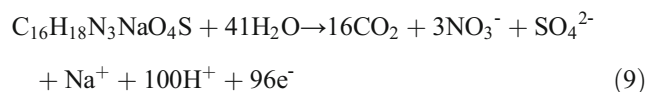
Analysis

The pH was measured with a Hanna Instruments pH-meter model HI8424. During electrolysis, samples were withdrawn from the solution kept in the cell at regular time intervals and then refrigerated at 4 °C until performing the analytical procedures.

The degree of mineralization was monitored from total organic carbon decay (TOC), which was determined with a Shimadzu Total Organic Carbon Analyzer (TOC 5000A). From these data, the mineralization current efficiency (MCE) for each treated solution was then calculated from Eq. (8) (Coria et al. 2016; García-Segura et al. 2016a, b; Salazar et al. 2016):

$$MCE(\%) = \frac{n \, F \, V_s \Delta(TOC)_{exp}}{4.32 \times 10^7 \, m \, I \, t} \times 100 \quad (8)$$

Where n is the number of electrons consumed in the mineralization of the corresponding antibiotic AMP; F is Faraday's constant (96487C mol^{-1}); Vs is the solution volume (L), (TOC)exp is the experimental TOC decay (mg L^{-1})

evaluated as the difference between the initial value and that analyzed at time t; 4.32×10^7 is a conversion factor (3600 s h^{-1} × 12000C mol^{-1}); I is the applied current (A); t is the electrolysis time (hours), and m corresponds to the 16 carbon atoms present in AMP. The n values were taken according to the mineralization reactions (Eq. (9)), considering a complete mineralization to CO$_2$, SO$_4^{2-}$, and NO$_3^-$ ions from the following reaction (96 e$^-$):

$$C_{16}H_{18}N_3NaO_4S + 41H_2O \rightarrow 16CO_2 + 3NO_3^- + SO_4^{2-}$$
$$+ Na^+ + 100H^+ + 96e^- \quad (9)$$

Aliquots were taken at different electrolysis times to evaluate the decay of the antibiotic concentration, which was analyzed by liquid chromatography in an HPLC Thermo Scientific coupled with an array detector diode Dionex Ultimate 3000, using a column Thermo Scientific Acclain C-18, 5 μm, 100 mm × 4.6 mm (id) at 25 °C ± 1°. Water/acetonitrile was used as mobile phase in a ratio of 80:20, respectively, at a flow of 0.5 mL min^{-1}. A calibration curve with different concentrations of AMP was prepared for the determination of the concentration of the antibiotic during the electrolysis. AMP presented a chromatographic peak with a retention time (rt) of 4.2 min.

The aliphatic carboxylic acids obtained as final products were identified and quantified by ion-exclusion chromatography using a Waters 625 Chromatograph with diode array detector 2966, fitted with a Bio-Rad Aminex HPX 87H, 30 cm × 7.8 mm (i.d.), column at 30 °C, at = 210 nm. The mobile phase was 4 mM H$_2$SO$_4$ at 0.6 mL min^{-1}. The corresponding calibration curves were constructed using pure acid standards. Absorption peaks with rt of 6.4 min for oxalic, 7.8 min for maleic, 9.3 min for oxamic, 13.6 min for formic, 14.8 min for acetic, and 15.3 min fumaric acid were obtained in the corresponding chromatograms. Released inorganic ions were quantified by a photometric technique. The formation of NO$_3^-$ was determined with nitrate reagent HI93728-0 and the formation of NH$_4^+$ with ammonia MR reagent (2 × 20 mL) HI93715-01, both from Hanna Instruments. Both ions were measured in a Hanna Instruments HI83099 Multiparameter photometer.

Aromatic intermediates were detected by UHPLC–MS/MS Ultimate 3000. Solutions of AMP were electrolyzed at short and long electrolysis times. Then, they were mixed until 300 mL were obtained, and extracted three times with 30 mL of CH$_2$Cl$_2$ and ethyl acetate for each extraction, with the purpose of identifying as many reaction intermediates as possible. The collected organic solution (90 mL) was dried with anhydrous Na$_2$SO$_4$, filtered and completely evaporated in a rotary evaporator, and then concentrated with methanol. Liquid chromatography electrospray ionization mass spectrometry (LC-ESI–MS) was performed

using a LTQ XL linear ion trap (Thermo Scientific) interfaced with a Thermo Scientific UHPLC system equipped with a quaternary pump (UltiMate 3000 High-Speed LC System). Sample separation was conducted on a Thermo Scientific MS C18 Kinetex (100×3 mm, 1.7 μm, 100 Å). Chromatographic analyses were carried out using isocratic elution A:B 30:70 with eluent A being formic acid (0.1% in MiliQ water) and eluent B consisting of formic acid (0.1% in MeOH J. T. Baker). The flow rate was 0.4 mL min^{-1} and the column temperature was maintained at 25 °C. The ESI source was set in positive ion detection mode. Full scan MS data were collected for a mass range of 100–2000 m/z.

Accumulation of H_2O_2 was determined by the method of formation of the ammonium metavanadate complex. An aliquot of 500 μL from the reactor was added to a plastic cell containing 500 μL of solution of ammonium metavanadate (6.2 mM). After 5 min, the absorbance at 450 nm was measured in a Genesys spectrophotometer.

Antimicrobial activity (AA) was determined by analyzing the inhibition zone in the agar diffusion test, using *Staphylococcus aureus* ATCC 6538 as the indicator microorganism. Twenty microliters of the sample solution was seeded on Petri dishes containing 5 mL of potato dextrose agar and 10 mL of nutrient agar inoculated with 10 μL of *S. aureus* (with an optical density of 0.600 at 580 nm). After 24 h at 37 °C in a Memmert (Schwabach) incubator, confluent bacterial growth was observed, and the diameter of the inhibitory halo was measured with a meter foot. All antimicrobial activity analyses were conducted at least by duplicate to ensure the reproducibility of methodology.

Results and discussion

Electrochemical degradation of AMP

A kinetic study of the degradation of the antibiotic ampicillin was carried out comparing different electrochemical advanced oxidation processes such as EO-H_2O_2, EF, and PEF. Moreover, photolysis process was applied to verify if UV radiation in conjunction with Fe^{2+} influenced in the degradation of the antibiotic. These experiments were performed under a concentration of 50 mg L^{-1} in 0.05 M Na_2SO_4 with 1 mg L^{-1} Fe^{2+} (for the EF and PEF experiments) in 0.250 L solution at pH 2.8.

Figure 1a shows the change in the concentration of AMP during the application for each process. It is possible to observe that when the system is irradiated with UV light in the presence of Fe^{2+} and without applying current, the concentration of AMP remains constant during 120 min of electrolysis, which means that the drug was not photolyzed. Then, removal of 68 and 73% of the antibiotic from the solution was reached
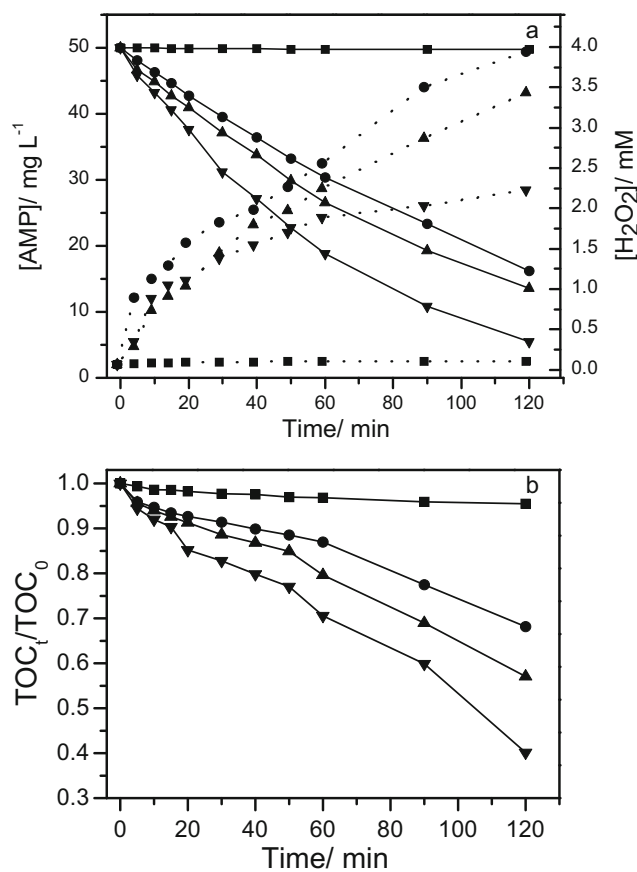

Fig. 1 **a** Degradation of 50 mg L^{-1} of AMP and evolution of hydrogen peroxide applying 5 mA cm^{-2}. Experimental conditions: 250 mL of solution containing Fe^{2+} [1 mg L^{-1}] and Na_2SO_4 [0.05 M], at pH 2.8 and 30 °C. (■) Photolysis/Fe^{2+}/365 nm, (●) EO-H_2O_2, H_2O_2, (▲) EF and (▼) PEF/365 nm, H_2O_2. **b** TOC decay at the same experimental conditions

through EO-H_2O_2 and EF after 120 min of electrolysis. However, a higher percentage of degradation (89%) was achieved with the PEF process after 120 min of electrolysis applying the same 5 mA cm^{-2}. These results could be explained by the hydroxyl radicals generated: (i) in the surface of the BDD anode, (ii) within the solution by the Fenton reaction, and (iii) those that are induced by the photolytic action by photo-reducing and photo-decarboxylating the Fe^{3+} complexes (Moreira et al. 2015; Pérez et al. 2017a, b).

For all the electrochemical processes carried out (EO-H_2O_2, EF and PEF), the degradation of the AMP follow a pseudo-first-order kinetic decay (SM2). The apparent rate constants were obtained from the slopes of graph $\ln[AMP]_0/[AMP]_t$. These values allowed us to affirm that the rate of degradation depends on the process, with differences of two times between EO-H_2O_2 and PEF processes: EO-H_2O_2 9.15×10^{-3} s^{-1} < EF 1.07×10^{-2} s^{-1} < PEF 1.81×10^{-2} s^{-1}.

The percentage of mineralization of the pollutant in solution in the different electrochemical processes applied was quantified by the decay of the total organic carbon. In Fig. 1b, it was not possible to observe a mineralization by

irradiating the solution with the sole action of UV light. Then, when EO-H$_2$O$_2$ and EF were applied, a mineralization of 32 and 43% were reached after 120 min, respectively (Fig. 1b). In contrast, when PEF was applied, a 63% TOC was removed in 120 min, evidencing the strong positive action of UV light supplied by lamp to photolyze Fe(III)-carboxylate complexes from Eq. (6), which remain in solution in EF since they are not attacked by hydroxyl radicals. According to these results, it was not possible to reach a higher percentage of mineralization applying a current density of 5 mA cm^{-2} in 120 min of electrolysis in PEF due to the generation of intermediates and short-chain carboxylic acids that persisted during electrolysis and reacted more slowly with the hydroxyl radical.

In the same way of both, AMP decay and TOC abatement, antimicrobial activity decreased mostly when the PEF process was applied. Figure 2 shows that, when irradiating the system with UV$_{365nm}$ light and in the presence of Fe^{2+}, the antimicrobial activity persisted during 120 min, which is in agreement with the not removal of the antibiotic (Fig. 1a). However, when performing the electrochemical process, it was possible to observe that AA decreased over electrolysis time in the cases of EO-H$_2$O$_2$, EF, and PEF, revealing that the antibiotic had been degraded. The EO-H$_2$O$_2$ and EF processes presented a 30 and 60% elimination of AA after 120 min remaining in a solution of 16.1 and 13.6 mg L^{-1} of AMP, respectively, as showed in Fig. 1a. In contrast, by PEF process was able to remove 90% of the AA after 120 min remaining in a 5.4-mg L^{-1} AMP solution, as observed in Fig. 1a. Authors like Giraldo-Aguirre et al. 2015a, band Serna-Galvis et al. 2016a, b report that this elimination of antimicrobial activity is caused by the rupture of the β-lactam ring that is part of the 6-aminopenicillanic acid structure, which is essential for the biological activity of these compounds. Therefore, the intermediates that are generated during the antibiotic degradation process do not present antimicrobial activity.
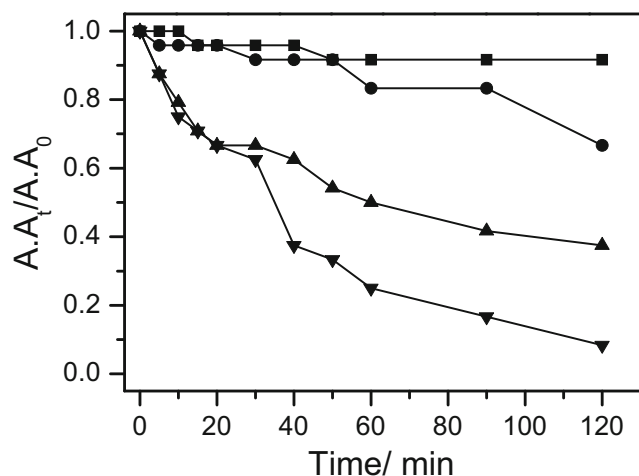

Fig. 2 AMP antimicrobial activity under the same experimental conditions of Fig. 1
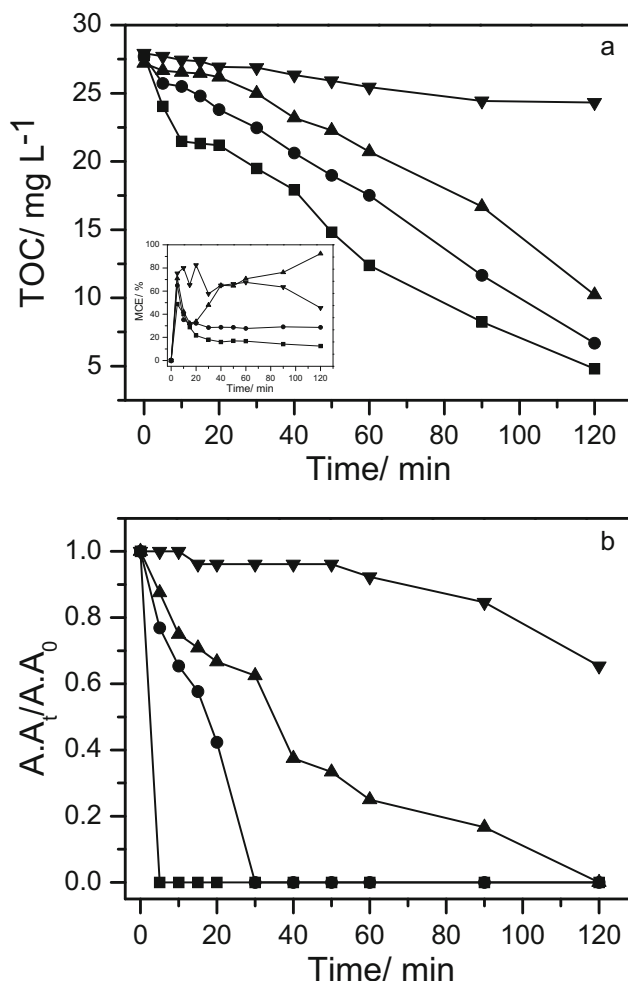

Fig. 3 **a** Effect of current density over AMP degradation and **b** AMP antimicrobial activity by PEF treatment. Two hundred fifty milliliters of AMP 50 mg L^{-1}, Fe^{2+} [1 mg L^{-1}], pH 2.8, 30 °C, Na$_2$SO$_4$ [0.05 M]: (▼) 2 mA cm^{-2}, (▲) 5 mA cm^{-2}, (●) 20 mA cm^{-2} and (■) 50 mA cm^{-2}. Inset: Effect of current density on mineralization current efficiency in PEF treatment

Influence of current density on the degradation of AMP by photoelectro-Fenton process
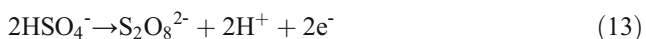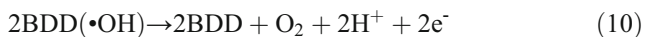
The velocity of the electrochemical reactions depends mainly on the current density applied to the system, which regulates the generation of species generated at the anode and cathode. For these experiments, different current densities were applied in a range from 2 to 50 mA cm^{-2} to a solution of 50 mg L^{-1} of AMP in 0.05 M Na$_2$SO$_4$ at pH 2.8 and at room temperature, with a concentration of Fe^{2+} of 1.0 mg L^{-1} using photoelectro-Fenton process.

Figure 3a shows a marked dependence on the removal of TOC after the increase of current density. When a current density of 2 mA cm^{-2} was applied, it was possible to remove 12% of the total organic carbon present in the solution in 120 min. When the current density was increased to 5, 20, and 50 mA cm^{-2}, 63, 78, and 86% of

TOC removal was reached in 120 min, respectively. This increase in the abasement of the total organic carbon over time was mainly due to the greater amount of hydroxyl radicals formed on the surface of the BDD electrode. Similarly, the concentration of H_2O_2 electrogenerated at the cathode also increased and lead to an increase in the amount of hydroxyl radicals formed in the solution by the Fenton reaction.

Figure 3b shows the dependence between the applied current density and AA removal during electrolysis time when PEF was applied. At a low current density, 30% of AA was removed after 120 min. Furthermore, when increasing current density to 5 mA cm^{-2}, AA decays at 120 min. Likewise, when applying a j of 20 and 50 mA cm^{-2}, the inhibition halo disappears at 30 and 5 min of electrolysis. According to these results, the elimination of AMP was complete after applying current densities between 5 and 50 mA cm^{-2}. Although the mineralization of AMP did not exceed 86% at high current densities as shown in Fig. 3a, these results highlight that intermediate products generated in the degradation of the antibiotic did not exhibit antimicrobial activity, because no halo of inhibition was observed until the end of the different experiments.

Based on the data shown in Fig. 3a, the mineralization current efficiency (MCE) for the degradation of AMP was determined using the PEF treatment. Insert in Fig. 3a shows that at 20 min of electrolysis, a maximum efficiency is reached with a value of 85% for 2 mA cm^{-2}. However, this efficiency decreases considerably over time and this was reflected in the low removal of the TOC at the end of the electrolysis. Similarly, insert in Fig. 3a shows 90% efficiency was achieved at a current density of 5 mA cm^{-2} in 120 min of electrolysis and with a high percentage of mineralization (63%). Then, when applying a current density over 20 mA cm^{-2}, the efficiency in current decreased notably. This happens because the activation energy of reactions occurring in parallel was exceeded, which does not favor the degradation and mineralization of organic contaminants, such as oxygen evolution by the hydroxyl radical via Eq. (10) or destruction with hydrogen peroxide and Fe^{2+} via Eqs. (11) and (12), respectively. Additionally, other reactions that lower the efficiency of the process, such as the production of $S_2O_8^{2-}$ and ozone by Eqs. (13) and (14), might occur (Sirés et al. 2014; Moreira et al. 2017).

$$2BDD(\bullet OH) \rightarrow 2BDD + O_2 + 2H^+ + 2e^- \qquad (10)$$

$$H_2O_2 + \bullet OH \rightarrow HO_2\bullet + H_2O \qquad (11)$$

$$Fe^{2+} + \bullet OH \rightarrow Fe^{3+} + {}^-OH \qquad (12)$$

$$2HSO_4^- \rightarrow S_2O_8^{2-} + 2H^+ + 2e^- \qquad (13)$$

$$3H_2O \rightarrow O_3 + 6H^+ + 6e^- \qquad (14)$$

Degradation of different initial concentrations of AMP by photoelectro-Fenton process

The oxidation capacity of the photo electro-Fenton process was studied to visualize the time needed to mineralize AMP with different levels of concentration. In the previous section, the effect of current density on the degradation of AMP in solution by means of PEF was studied. Consequently, MCE was calculated, and results showed that the highest efficiency was obtained by applying a current density of 5 mA cm^{-2}. With the chosen current density, different solutions containing 10 to 100 mg L^{-1} of AMP in 0.05 M Na$_2$SO$_4$ with 1 mg L^{-1} of Fe^{2+} at pH 2.8 were evaluated. Figure 4a shows that at high concentrations of 100 and 75 mg L^{-1} of AMP, it was possible to mineralize only 30 and 29% in both cases, which could be improved by increasing electrolysis time. However, when low initial concentrations of AMP (50 and 10 mg L^{-1}) were used, of 62 and 55% mineralization was achieved, respectively. The incomplete mineralization in some cases implies that intermediate compounds
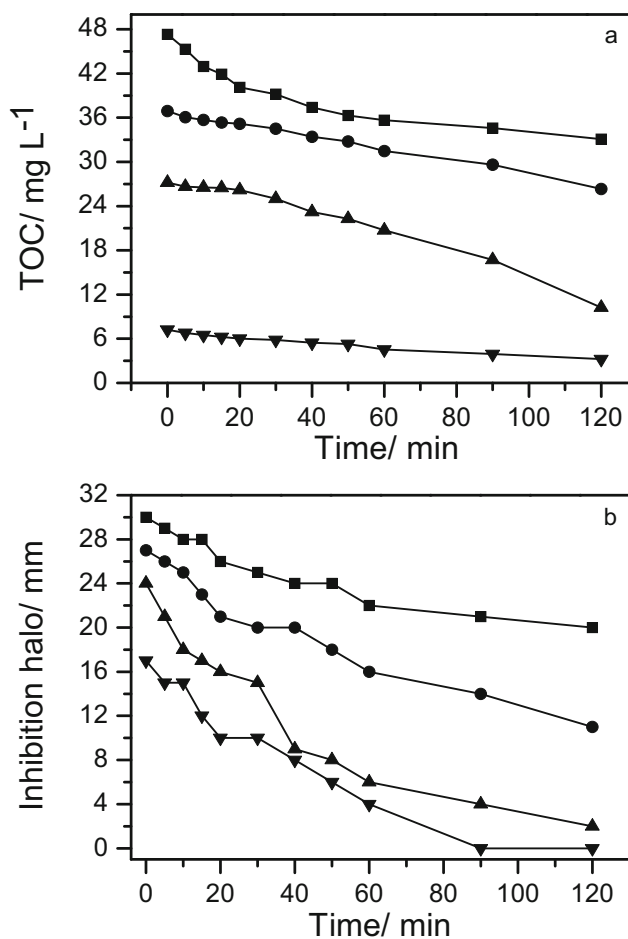
Fig. 4 **a** Effect of the initial AMP concentration. **b** AMP antimicrobial activity by PFE treatment. Two hundred fifty milliliters of AMP [50 mg L^{-1}], Fe^{2+} [1 mg L^{-1}], pH 2.8, 30 °C, Na$_2$SO$_4$ [0.05 M]: (■) 100 mg L^{-1}, (●) 75 mg L^{-1}, (▲) 50 mg L^{-1} and (▼) 10 mg L^{-1}

generated during the AMP degradation process are persistent at the end of the process.

The antimicrobial activity in solutions with different concentrations of AMP was evaluated during the process of antibiotic degradation by means of PEF (Fig. 4b). The results showed that at low initial concentrations of AMP (10 mg L^{-1}), the antimicrobial activity was eliminated in 90 min of electrolysis; however, the percentage of mineralization was 55%, as shown in Fig. 4a, which means that intermediate products formed during antibiotic degradation but with no AA persist in solution. When initial concentrations of AMP between 50 and 100 mg L^{-1} were used, antimicrobial activity still persisted at 120 min of electrolysis, which could be improved by increasing electrolysis time.

According to the mineralization data displayed in Fig. 4a, MCE in AMP degradation was obtained at different initial concentrations during 120 min of electrolysis (data not shown). Two hundred eighty-one percent efficiency in antibiotic mineralization was achieved at 10 min of electrolysis, which then decreases at 120 min of experiment, a behavior that coincides with the low percentage of mineralization obtained at 2 h of electrolysis. In the same line, the efficiency obtained with an initial AMP concentration of 75 mg L^{-1} increases by 110% at 5 min of electrolysis, but decreases over time, remaining constant until the end of the process with a low pollutant mineralization. Nevertheless, when a solution with a concentration of 50 mg L^{-1} was electrolyzed, maximum efficiency was reached at 120 min, which increased in the course of electrolysis and was reflected in the high percentage of mineralization obtained at the end of the experiment. Finally, when the initial concentration of the solution was 10 mg L^{-1}, the MCE had a 57% increase at 5 min of experiment and then decreased until 120 min of electrolysis, due to the lower amount of antibiotic in solution compared to the greater amount of oxidizing species that were generated in the process, which implies a loss in efficiency, because these oxidants can react with other species giving rise to parasite reactions (El-Ghenymy et al. 2013). Additionally, a percentage of mineralization over 50% was obtained.

On the other hand, two degradation experiments of AMP using real micro pollutant concentration (10 and 50 μg L^{-1}) were performed in 0.05 M Na_2SO_4 with 1 mg L^{-1} of Fe^{2+} at pH 2.8. A total degradation and mineralization of the drug was achieved after 8–10 min of electrolysis evidencing that, by PEF process is possible to degrade AMP in concentrations at environmental level.

Intermediates and products generated during the degradation of AMP by PEF

The AMP solutions degraded through PEF by applying a current density of 5 mA cm^{-2} were also analyzed by ion-exclusion HPLC to qualitatively identify the short-chain carboxylic acids generated during the studied mineralization process. The chromatograms revealed peaks related to maleic, oxalic, oxamic, formic, acetic, and fumaric acids. The carboxylic acids generated during the mineralization process, such as the evolution of maleic and fumaric acid, may be a consequence of the fragmentation of the aromatic rings present in the molecule of the antibiotic (Ruiz et al. 2011; Almeida et al. 2012). These two formed acids can continue to be attacked by hydroxyl radicals, thereby evolving to simpler carboxylic acids, such as acetic, oxalic, and formic acids. Finally, the formation of oxamic acid is caused by the destruction of the molecule zones where these acids are derivatives of nitrogen. Formic acid and oxamic acid can be mineralized directly to CO_2 (Thiam et al. 2015; Wang et al. 2011).
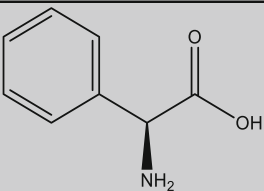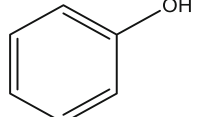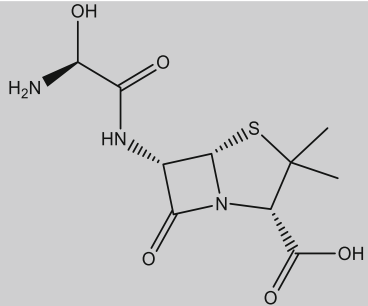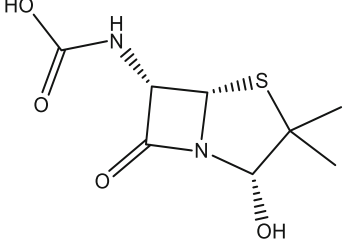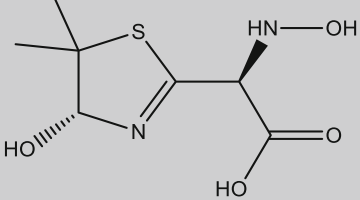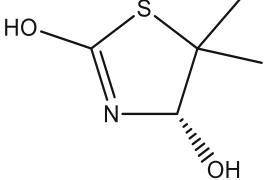
The inorganic ions produced during the degradation of AMP at 5 mA cm^{-2} in the PEF process were identified by photometry. When the antibiotic in solution is degraded, nitrogenous species are generated, because the antibiotic presents nitrogenous groups in its structure. The ions identified are the ammonium ion (NH_4^+) and the nitrate ion (NO_3^-), being these species completely oxidized and possibly being generated in a high concentration.

Therefore, mainly nitrate ions could be generated in a greater proportion than ammonium ions by means of the oxidation of the antibiotic, whose reaction is expressed in Eq. (9).

In order to establish a possible mechanism for the degradation of the antibiotic AMP by photo electro-Fenton, we have identified the main reaction intermediates. Identification of aromatic intermediates was carried out using UHPLC-MS/MS. During antibiotic electrolysis, seven possible structures associated with oxidation compounds were detected and can be observed together with their masses in Table 1.

Based on the products detected in this work, a possible mineralization pathway is shown in Fig. 5 for the degradation of the antibiotic AMP (compound 1) by PEF. The formation of aromatic compounds is attributed to successive attacks of ·OH on the antibiotic and its intermediates. In a first step, AMP generated two intermediates due to the attack of the hydroxyl radical on the amide group, dividing the molecule into two parts: compound 2, whose m/z is 151.16 and compound 4, whose m/z is 289.30. Following the first reaction pathway, compound 2 is attacked by hydroxyl radicals by breaking the bond between the C1 of benzene and its substituent, giving rise to compound 3, whose m/z is 94.11. Besides, through compound 4, compound 5, whose m/z is 232.25, is generated. Compound 5 is formed by two hydroxylations, one on the carbonyl of the amide and the other on the substituted carbon of the thiazolidine ring by a carboxylic group. As in the latter path, compound 5 is now attacked by ·OH, generating the breakdown of the betalactam ring and breaking the bond between the carbonyl and the nitrogen of the aliphatic chain,

Table 1 Aromatics and hydroxylated derivatives identified by UHPLC–MS/MS for antibiotic ampicillin

Compound	Chemical structure	Name	m/z
2		(S)-2-amino-2-phenylacetic acid	151.16
3		Fenol	94.11
4		(2S,5S,6S)-6-((S)-2-amino-2-hydroxyacetamido)-3,3-dimethyl-7-oxo-4-thia-1-azabicyclo[3.2.0]heptane-2-carboxylic acid	289.30
5		((2S,5S,6S)-2-hydroxy-3,3-dimethyl-7-oxo-4-thia-1-azabicyclo[3.2.0]heptan-6-yl)carbamic acid	232.25
6		(S)-2-((R)-4-hydroxy-5,5-dimethyl-4,5-dihydrothiazol-2-yl)-2-(hydroxyamino)acetic acid	220.24
7		(R)-5,5-dimethyl-4,5-dihydrothiazole-2,4-diol	147.19

thereby forming compound 6, whose *m/z* is 220.24. Finally, compound 7, whose *m/z* is 147.19, is detected after being generated by the hydroxylation of compound 6 on the carbon double bonded to nitrogen.

On the other hand, the rupture of aromatic rings produces higher molecular weight acids such as maleic or fumaric, and then acids of lower molecular weight. These acids are attacked by hydroxyl radicals, generating oxalic, oxamic, and formic acids, which can react with the Fe^{3+} in solution and form iron complexes that undergo photodecarboxylation, regenerating

Fe^{2+} prior to the complete mineralization to CO_2 and mineralization confirming inorganic ions.

Degradation of AMP in a real wastewater by PEF

The removal of AMP was performed in a real industrial wastewater from a Slaughterhouse company and the results are shown in Fig. 6. Two hundred fifty milliliters of industrial wastewater was spike with 50 mg L^{-1} of AMP and treated by PEF applying a current density of 5 mA cm^{-2}, in the

Fig. 5 Pathway proposed for the mineralization of the antibiotic ampicillin by PEF treatment
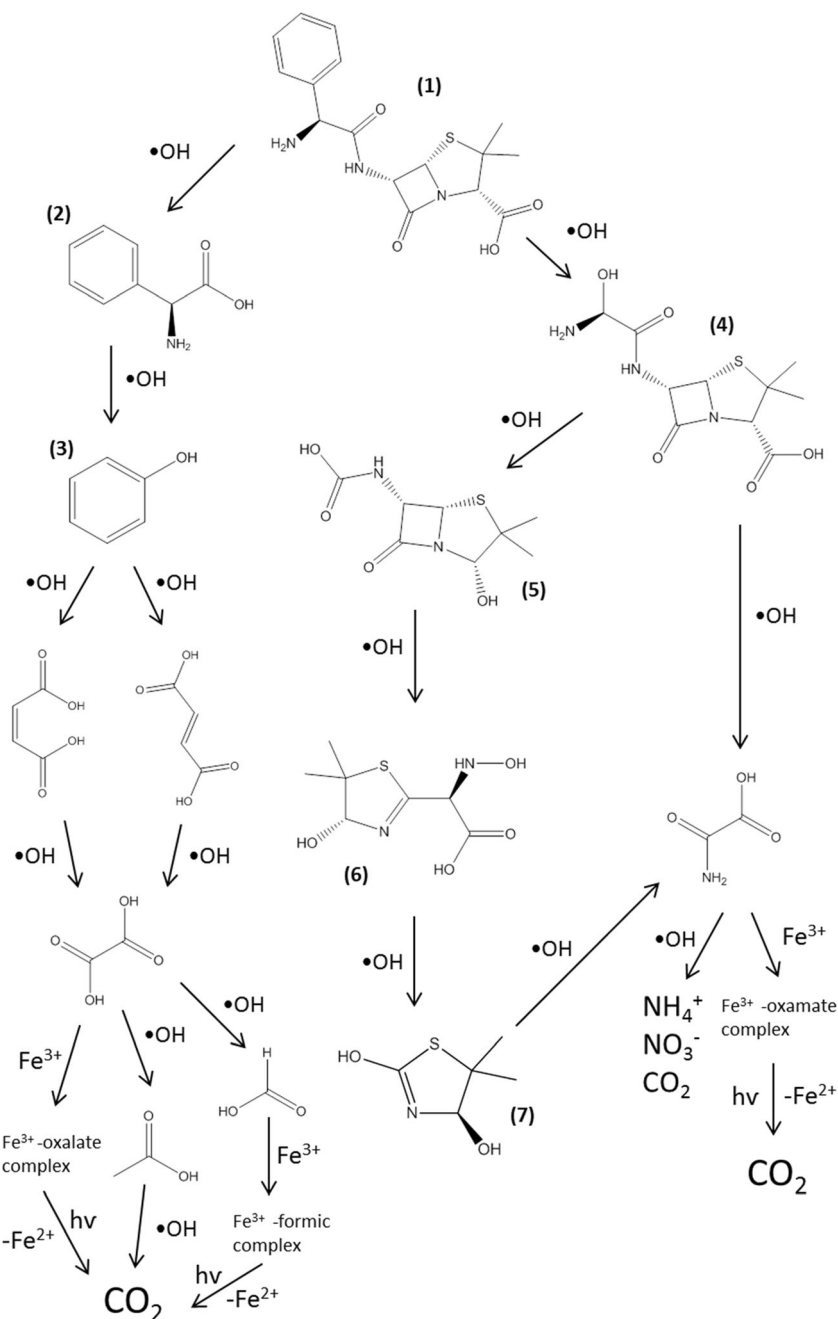
presence of 1 mg L^{-1} of Fe^{2+} and 0.05 M Na_2SO_4 at pH 2.8 and 30 °C. Almost a complete degradation of AMP was obtained after 60 min of electrolysis, evidencing that, in a complex matrix, the PEF method is effective in the elimination of this kind of pollutant. In the same way, % of removal of TOC and DQO increases with the electrolysis time, which implies that not only the degradation of AMP occurs due to the hydroxyl radicals generated during the photoelectro-Fenton process, but also those organic components present in the real sample. On the other hand, a complete elimination of the turbidity is achieved after 3 h of treatment. All these results allow to obtain a treated water that complies with Chilean standards for the elimination of industrial wastewater (DS 609, 1998).

Conclusions

It was determined that the antibiotic AMP can be degraded and mineralized by PEF using a BDD anode, air diffusion cathode, and exposing the solutions to UV_{365nm} radiation due to hydroxyl radicals generated in the bulk, on the anode surface and UV radiation. In addition, the direct photolysis of complexes between Fe^{3+} and some organic intermediates led
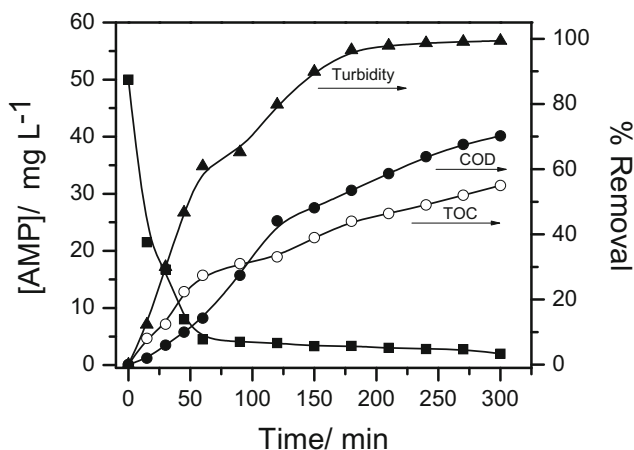
Fig. 6 TOC, COD, turbidity, and concentration abatement of 50 mg L^{-1} of AMP in a real matrix of from a Slaughterhouse Company post biological treatment by PFE. Experimental condition: 250 mL of wastewater, current density 5 mA cm^{-2}, Fe^{2+} [1 mg L^{-1}], Na_2SO_4 [0.05 M], pH 2.8 and 30 °C

to the fastest reaction rates. Together with the degradation of AMP, the antimicrobial activity in the solution was eliminated after 120 min of electrolysis. PEF allows greater decay of the antibiotic concentration, TOC decay, complete elimination of antimicrobial activity, and process efficiency over other electrochemical processes such as EO-H_2O_2 and EF. The decay of the concentration of the antibiotic follows pseudo-first-order kinetics, and it is possible to reach almost total degradation of AMP in a real complex matrix of wastewater.

Finally, during the degradation of the antibiotic, aromatic compounds, carboxylic acids, and inorganic ions are produced prior to the transformation into CO_2.

References

Abdessalem AK, Bellakhal N, Oturan N, Dachraoui M, Oturan MA (2010) Treatment of a mixture of three pesticides by photo- and electro-Fenton processes. Desalination 250:450–455

Almeida LC, García-Segura S, Arias C, Bocchi N, Brillas E (2012) Electrochemical mineralization of the azo dye Acid Red 29 (Chromotrope 2R) by photoelectro-Fenton process. Chemosphere 89:751–758

Annabi C, Fourcade F, Soutrel I, Geneste F, Floner D, Bellakhal N, Amrane A (2016) Degradation of enoxacin antibiotic by the electro-Fenton process: optimization, biodegradability improvement and degradation mechanism. J Environ Manag 165:96–105

Anotai J, Singhadech S, Su C, Lu M (2011) Comparison of o-toluidine degradation by Fenton, electro-Fenton and photoelectro-Fenton processes. J Hazard Mater 196:395–401

Babuponnusami A, Muthukumar K (2012) Advanced oxidation of phenol: a comparison between Fenton, electro-Fenton, sono-electro-Fenton and photo-electro-Fenton processes. Chem Eng J 183:1–9

Bedolla-Guzmán A, Sirés I, Thiam A, Peralta-Hernández JM, Gutiérrez-Granados S, Brillas E (2016) Application of anodic oxidation, electro-Fenton and UVA photoelectro-Fenton to decolorize and mineralize acidic solutions of Reactive Yellow 160 azo dye. Electrochim Acta 206:307–316

Benito A, Penadés A, Lliberia JL, González-Olmos R (2017) Degradation pathways of aniline in aqueous solutions during electro-oxidation with BDD electrodes and UV/H_2O_2 treatment. Chemosphere 166:230–237

Chávez I, Arias C, Cabot PL, Centellas F, Rodríguez RM, Garrido JA, Brillas E (2010) Mineralization of the drug β-blocker atenolol by electro-Fenton and photoelectro-Fenton using an air-diffusion cathode for H2O2 electrogeneration combined with a carbon-felt cathode for Fe2+ regeneration. Appl Catal B Environ 96:361–369

Coria G, Sirés I, Brillas E, Nava JL (2016) Influence of the anode material on the degradation of naproxen by Fenton–based electrochemical processes. Chem Eng J 304:817–825

Cruz-Rizo A, Gutiérrez-Granados S, Salazar R, Peralta-Hernández JM (2017) Application of electro-Fenton/BDD process for treating tannery wastewaters with industrial dyes. Sep Purif Technol 172:296–302

Decreto Supremo 609 (1998) Chile: Ministerio Secretaría General de la Presidencia

de Luna MDG, Veciana ML, Su CC, Lu M-C (2012) Acetaminophen degradation by electro-Fenton and photoelectro-Fenton using a double cathode electrochemical cell. J Hazard Mater 217–218:200–207

Díez AM, Iglesias O, Rosales E, Sanromán MA, Pazos M (2016) Optimization of two-chamber photo electro Fenton reactor for the treatment of winery wastewater. Process Saf Environ Prot 101:72–79

El-Ghenymy A, Cabot PL, Centellas F, Garrido JA, Rodríguez RM, Arias C, Brillas E (2013) Mineralization of sulfanilamide by electro-Fenton and solar photoelectro-Fenton in a pre-pilot plant with a Pt/air-diffusion cell. Chemosphere 91:1324–1331

El-Ghenymy A, Centellas F, Rodríguez RM, Cabot PL, Garrido JA, Sirés I, Brillas E (2015) Comparative use of anodic oxidation, electro-Fenton and photoelectro-Fenton with Pt or boron-doped diamond anode to decolorize and mineralize Malachite Green oxalate dye. Electrochim Acta 182:247–256

Espinoza C, Romero J, Villegas L, Cornejo-Ponce L, Salazar R (2016) Mineralization of the textile dye acid yellow 42 by solar photoelectro-Fenton in a lab-pilot plant. J Hazard Mater 319:24–33

Feng L, van Hullebusch ED, Rodrigo MA, Esposito G, Oturan MA (2013) Removal of residual anti-inflammatory and analgesic pharmaceuticals from aqueous system by electrochemical advanced oxidation processes. A review. Chem Eng J 228:944–964

García-Rodríguez O, Bañuelos JA, El-Ghenymy A, Godínez LA, Brillas E, Rodríguez-Valadez FJ (2016) Use of a carbon felt–iron oxide air-diffusion cathode for the mineralization of Malachite Green dye by heterogeneous electro-Fenton and UVA photoelectro-Fenton processes. J Electroanal Chem 767:40–48

García-Segura S, El-Ghenymy A, Centella F, Rodríguez RM, Arias C, Garrido JA, Cabot PL, Brillas E (2012) Comparative degradation of the diazo dye Direct Yellow 4 by electro-Fenton, photoelectro-Fenton and photo assisted electro-Fenton. J Electroanal Chem 681:36–43

García-Segura S, Salazar R, Brillas E (2013) Mineralization of phthalic acid by solar photoelectro-Fenton with a stirred boron-doped diamond/air-diffusion tank reactor: influence of Fe^{3+} and Cu^{2+}

catalysts and identification of oxidation products. Electrochim Acta 113:609–619

García-Segura S, Brillas E, Cornejo-Ponce L, Salazar R (2016a) Effect of the Fe^{3+}/Cu^{2+} ratio on the removal of the recalcitrant oxalic and oxamic acids by electro-Fenton and solar photoelectron-Fenton. Sol Energy 124:242–253

García-Segura S, Silva Lima A, Bezerra Cavalcanti E, Brillas E (2016b) Anodic oxidation, electro-Fenton and photoelectro-Fenton degradation of pyridinium- and imidazolium-based ionic liquids in waters using a BDD/air diffusion cell. Electrochim Acta 198:268–279

García-Segura S, Anotai J, Singhadech S, Lu M-C (2017) Enhancement of biodegradability of o-toluidine effluents by electro-assisted photo-Fenton treatment. Process Saf Environ Prot 106:60–67

Giraldo-Aguirre L, Erazo-Erazo ED, Flórez-Acosta OA, Serna-Galvis EA, Torres-Palma RA (2015a) Degradation of the antibiotic oxacillin in water by anodic oxidation with Ti/IrO_2 anodes: evaluation of degradation routes, organic by-products and effects of water matrix components. Chem Eng J 279:103–114

Giraldo-Aguirre L, Erazo-Erazo ED, Flórez-Acosta OA, Serna-Galvis EA, Torres-Palma RA (2015b) TiO_2 photocatalysis applied to the degradation and antimicrobial activity removal of oxacillin: evaluation of matrix components, experimental parameters, degradation pathways and identification. J Photochem Photobiol A Chem 311: 95–103

Katzung BG, Masters SB, Trevor AJ, (2013) Farmacología Básica y Clínica, Mc Graw Hill 12th edición

Kemper N (2008) Veterinary antibiotics in the aquatic and terrestrial environment. Ecol Indic 8:1–13

Kummerer K (2009) The presence of pharmaceuticals in the environment due to human use-present knowledge and future challenges. J Environ Manag 90:2354–2366

Liu S, X-r Z, H-y S, R-p L, Y-f F, Y-p H (2013) The degradation of tetracycline in a photo-electro-Fenton system. Chem Eng J 231: 441–448

Masomboon N, Ratanatamskul C, Lu M-C (2010) Mineralization of 2,6-dimethylaniline by photoelectron-Fenton process. Appl Catal A Gen 384:128–135

Moreira FC, García-Segura S, Boaventura RAR, Brillas E, Vilar VJP (2014) Degradation of the antibiotic trimethoprim by electrochemical advanced oxidation processes using a carbon-PTFE air-diffusion cathode and a boron-doped diamond or platinum anode. Appl Catal B Environ 160–161:492–505

Moreira FC, Boaventura RAR, Brillas E, Vilar VJP (2015) Degradation of trimethoprim antibiotic by UVA photoelectro-Fenton process mediated by Fe(III)-carboxylate complexes. Appl Catal B Environ 162: 34–44

Moreira FC, Boaventura RAR, Brillas E, Vilar VJP (2017) Electrochemical advanced oxidation processes: a review on their application to synthetic and real wastewater. Appl Catal B Environ 202:217–261

Olvera-Vargas H, Oturan N, Oturan MA, Brillas E (2015) Electro-Fenton and solar photoelectro-Fenton treatments of the pharmaceutical ranitidine in pre-pilot flow plant scale. Sep Purif Technol 146:127–135

Pereira GF, El-Ghenymy A, Thiam A, Carlesi C, Eguiluz KIB, Salazar-Banda GR, Brillas E (2016) Effective removal of Orange-G azo dye from water by electro-Fenton and photoelectro-Fenton processes using a boron-doped diamond anode. Sep Purif Technol 160:145–151

Pérez JF, Llanos J, Sáez C, López P, Cañizares P, Rodrigo MA (2017a) Treatment of real effluents from the pharmaceutical industry: a comparison between Fenton oxidation and conductive-diamond electro-oxidation. J Environ Manag 195:216–223

Pérez T, Sirés I, Brillas E, Nava JL (2017b) Solar photoelectro-Fenton flow plant modeling for the degradation of the antibiotic erythromycin in sulfate médium. Electrochim Acta 2017:45–56

Ruiz EJ, Arias C, Brillas E, Hernández-Ramírez A, Peralta-Hernández JM (2011) Mineralization of acid yellow 36 azo dye by electro-Fenton and solar photoelectro-Fenton processes with a boron-doped diamond anode. Chemosphere 82:495–501

Salazar R, García-Segura S, Ureta-Zañartu MS, Brillas E (2011) Degradation of disperse azo dyes from waters by solar photoelectro-Fenton. Electrochim Acta 56:6371–6379

Salazar C, Contreras N, Mansilla HD, Yánez J, Salazar R (2016) Electrochemical degradation of the antihypertensive losartan in aqueous medium by electro-oxidation with boron-doped diamond electrode. J Hazard Mater 319:84–92

Sales Solano AM, García-Segura S, Martínez-Huitle CA, Brillas E (2015) Degradation of acidic aqueous solution of the diazo dye Congo Red by photo-assisted electrochemical processes based on Fenton's reaction chemistry. Appl Catal B Environ 168–169:559–571

Serna-Galvis EA, Silva-Agredo J, Giraldo-Aguirre AL, Torres-Palma RA (2015) Sonochemical degradation of the pharmaceutical fluoxetine: effect of parameters, organic and inorganic additives and combination with a biological system. Sci Total Environ 525:354–360

Serna-Galvis EA, Silva-Agredo J, Giraldo-Aguirre AL, Flórez-Acosta OA, Torres-Palma RA (2016a) Comparative study of the effect of pharmaceutical additives on the elimination of antibiotic activity during the treatment of oxacillin in water by the photo-Fenton, TiO_2-photocatalysis and electrochemical processes. Sci Total Environ 541:1431–1438

Serna-Galvis EA, Silva-Agredo J, Giraldo-Aguirre AL, Flórez-Acosta OA, Torres-Palma RA (2016b) High frequency ultrasound as a selective advanced oxidation process to remove penicillinic antibiotics and eliminate its antimicrobial activity from water. Ultrason Sonochem 31:276–283

Sirés I, Brillas E (2016) Electrochemical removal of pharmaceuticals from water streams: reactivity elucidation by mass spectrometry. TrAC Trends Anal Chem 70:112–121

Sirés I, Brillas E, Oturan MA, Rodrigo MA, Panizza M (2014) Electrochemical advanced oxidation processes: today and tomorrow. A review. Environ Sci Pollut Res 21:8336–8367

Thiam A, Sirés I, Brillas E (2015) Treatment of a mixture of food color additives (E122, E124 and E129) in different water matrices by UVA and solar photoelectron-Fenton. Water Res 81:178–187

Vidal J, Huiliñir C, Salazar R (2016) Removal of organic matter contained in slaughterhouse wastewater using a combination of anaerobic digestion and solar photoelectro-Fenton processes. Electrochim Acta 210:163–170

Wang A, Li Y-Y, Ledezma Estrada A (2011) Mineralization of antibiotic sulfamethoxazole by photoelectron-Fenton treatment using activated carbon filter cathode and under UVA irradiation. Appl Catal B Environ 102:378–386

Zazou H, Oturan N, Sonmez-Celebi M, Hamdani M, Oturan MA (2016) Mineralization of chlorobenzene in aqueous medium by anodic oxidation and electro-Fenton processes using Pt or BDD anode and carbon felt cathode. J Electroanal Chem 774:22–30